

Effective iterative algorithm for the Limit Analysis of truss-frame structures by a kinematic approach

Rosalba Ferrari^a, Giuseppe Cocchetti^{a,b}, Egidio Rizzi^{a,*}

^a Università degli Studi di Bergamo, Dipartimento di Ingegneria e Scienze Applicate, viale G. Marconi 5, I-24044 Dalmine (BG), Italy

^b Politecnico di Milano, Dipartimento di Ingegneria Civile e Ambientale, piazza L. da Vinci 32, I-20133 Milano, Italy



ARTICLE INFO

Article history:

Received 25 August 2017

Accepted 28 November 2017

Keywords:

Limit Analysis (LA)

Upper-bound (kinematic) theorem

Collapse load multiplier

Plastic collapse mechanism

Non-linear FEM model

Truss-frame structures

ABSTRACT

A former algorithm of Limit Analysis (LA) at the continuum mechanics scale by a kinematic, upper-bound approach is here re-interpreted in the realm of LA of large-scale 3D truss-frame structures and effectively implemented toward fast and convenient collapse load multiplier and mechanism evaluation. First, the algorithm is described in its iterative design, and convergence is demonstrated. Some initial applications to truss-frame test structures under bending and torsion are also discussed. Then, the algorithm is successfully applied to two benchmark multi-story frames. It is shown that very consistent and quick evaluations of the collapse characteristics are obtained by this direct method, in comparison to those provided by alternative classical mathematical programming approaches and much expensive evolutive step-by-step solutions of the whole structural elastoplastic response. The algorithm shows a superior performance, with the kinematic multiplier truly precipitating from above on the collapse one, in very few iterations, with a consistent associated estimation of the plastic collapse mechanism.

© 2017 Elsevier Ltd. All rights reserved.

1. Introduction

Limit Analysis (LA) constitutes by today a well-established and consolidated discipline, for evaluating consistent bounds on the collapse (limit) loads acting on engineering structures characterized by a mechanical behavior that may be idealized as perfectly plastic, subjected to increasing live loads. LA may be considered as a milestone in the more recent history of structural mechanics and provides a rather powerful tool for structural design and assessment purposes in a wide variety of engineering situations. It has acquired its rational formulation thanks to the contribution by Drucker et al. [1], who formulated and demonstrated the fundamental theorems of LA for a continuum. More recent consolidated contributions, such as those by Massonet and Save [2], Kaliszky [3], Lubliner [4] and Jirasek and Bazant [5], have further made the theory and methods of LA rather fundamental in the applications of mechanics of solids and structures, becoming by now classical references on the topic (see also contributions in Spiliopoulos and Weichert [6] and Foreword by G. Maier in it).

LA is a methodology characterized by intrinsic peculiarities that may be regarded as bringing considerable advantages in the

engineering practice. These include the fact that it determines safety coefficients with respect to the ultimate limit state of a structure and the kinematics of a collapse mechanism, providing essential and very expressive results to structural designers. For this reason, it appears as particularly suitable for comparative evaluations among different design options, in order to easily guide engineers toward selecting the most efficient and feasible structural choices.

LA provides theorems for the determination of the ultimate load of a perfectly plastic solid or a structure. The *lower bound theorem*, or equivalently the *static* (“safe”) *principle*, states that if, for a given set of loads, an equilibrium stress field (satisfying also the stress boundary conditions) can be found, which nowhere violates the yield condition, the body will not collapse. The *upper bound theorem*, or equivalently the *kinematic principle*, states that, for a given collapse mechanism whose kinematics is compatible, the ratio between the internal and external rates of dissipation will be higher than or equal to that actually found at collapse, thus providing an upper bound on the ultimate load. It is a well-known fact that, in both cases, the plastic behavior intrinsically renders the problem to be non-linear. Essentially, two different approaches are usually adopted to deal with this issue: (i) the use of a polyhedral approximation to the yield surface; (ii) the implementation of direct non-linear programming algorithms.

* Corresponding author.

E-mail address: egidio.rizzi@unibg.it (E. Rizzi).

The first approach actually consists of a linearization technique of the convex yield condition, through which the resulting problem reduces to classical Linear Programming (LP). Firstly introduced by Maier [7] and Lysmer [8], LP was applied to LA finalities using mainly two methods, i.e. the Simplex Method (see e.g. Capurso [9], Anderheggen and Knöpfel [10], Christiansen [11]) and, more recently, the Interior Point Methods (IPMs) (see e.g. Andersen and Christiansen [12]).

Later, advantages in mathematical programming have allowed to develop efficient techniques that make it possible to consider the intrinsic non-linearity of the problem. In the works by Andersen et al. [13,15] and Christiansen and Andersen [14], the IPM was developed and extended to be applied to non-linear programming algorithms, leading to approximations of both lower and upper bounds of the collapse multiplier. In Zouain et al. [16], a new non-linear programming approach was proposed for general LA problems in the form of a quasi-Newton optimization algorithm. The same algorithm was then adapted by Lyamin and Sloan [17,18] to obtain strict lower and upper bounds, respectively, for soil mechanics problems on uniform meshes. Formalizing the upper and the lower bound principles as a Second-Order Cone Programming (SOCP) problem (see Ben-Tal and Nemirovski [19] for presentation of conic programming), Ciria and Peraire [20] presented an efficient procedure that exploits the IPM to compute strict upper and lower bounds for the exact collapse load multiplier.

To the Authors' knowledge, except when LA was at its very beginnings, namely when it was based on techniques of bounding the critical load-carrying capacity of beams and frames (see e.g. Prager [21], and references quoted therein concerning the incipit of LA theory), discussions specifically targeted on LA of frames appear more sporadic and slightly translated in time with respect to LA of solids.

In the early 80s, Nguyen-Dang [22] developed a software (CEPAO) to treat Limit Analysis with proportional loading and shakedown analysis with repeated cyclic loading of 2D frames, by linearizing the N–M interaction yield surface. The method appeared then to have been extended to 3D steel frames more than twenty years later, using a 16-facet yield surface combining axial force and bending moments interaction, within a kinematic method using a Linear Programming technique (Van Long and Dang Hung [23]).

In the meantime, the rapid development of computer technology has enabled for further refined algorithms, to capture the inelastic behavior of frames with an increasing accuracy, thus moving the interest of researchers to topics more related to the evolutive response estimation of structures. Remaining in the case of the "line" element assumption, advantages have been focused on the degree of refinement on representing plastic yielding effects, both considering localized plastic hinge approaches (see e.g. Liew et al. [24], Liew et al. [25], Cocchetti and Maier [26], Tangaramvong and Tin-Loi [27]) and smeared plasticity approaches (see Chiorean and Barsan [33] and references cited therein).

After returning on the scene from ten years ago (Van Long and Dang Hung [23]), LA of frames has been revived in recent years with several interesting applications. For example, in Lógó et al. [34] the lower bound theorem has been applied to study the influence of semi-rigid connections on the plastic behavior of elasto-plastic steel frames subjected to dead load and quasi-static working loads. In Skordeli and Bisbos [35] LA of spatial steel frames has been translated into a SOCP problem, approximating the plastic yield surfaces related to the cross sections through ellipsoids. The method turned out rather efficient to comply with provisions from Eurocode 3. The same concept has then been extended to

composite frames by Bleyer and Buhan [36]. In Nikolaou et al. [37] a LP problem has been set to conduct LA of 2D frames considering foundation-structure interaction, taking into account the foundation load-carrying capacity.

This work presents an unprecedented direct non-linear programming algorithm for LA of truss-frames, which exploits a convenient reshaping of the internal power dissipation description of a beam element, in order to adapt an existing efficient approach originally presented by Zhang et al. [28] for LA of continua (later improved in Zhang et al. [29] to treat a combined action of constant loadings and proportional loadings), within the classical FEM analysis based on beam element discretization. The procedure, implemented through an efficient iterative algorithm, leads to a *quadratic formulation of the kinematic theorem*, which represents a necessary condition for the efficient functioning of the procedure. In the paper, specific reference is made to a Rankine-type boxed-form yield domain for describing the interaction among the internal static variables of a beam element.

The procedure may deserve attention for its both straightforward implementation and elevated speed of convergence, which has proven to display a saving of more than 90% of the computational time employed for a corresponding evolutive Limit Analysis of two exemplifying 3D truss-frame structures based on a step-by-step elastoplastic approach (Ferrari et al. [31,32]). Unlike for the direct method herein proposed, this latter evolutive approach relies on an iterative procedure in which the global elastoplastic matrix of a structure is iteratively updated, based on the plastic modes that become active during the increment of the live loads applied to the structure, in this way allowing for the characteristic non-linear load/displacement response curve estimation, up to collapse. In order to allow for the employment of the algorithm toward the effective modeling of the global non-linear elastoplastic behavior of large truss-frame structures, several peculiar features have been added to enrich such a procedure.

Notice that term "truss-frame" here refers to the fact that the considered structure may either reproduce a classical frame (i.e. like a multi-story one), as typically considered in benchmarking cases in the LA of beams and frames, or even resemble a frame morphologically displaying a trusswork geometrical assembly, and, moreover, potentially yielding also on the axial internal action, thus leading to the possibility of handling the LA also for true trusses with structural elements just pinned at the nodes.

The direct LA kinematic method proposed here is distinguished from other kinematic approaches due to its alternative and elegant formulation, which provides a very convenient procedure for the LA of truss-frames, able to bring back the formulation of the upper-bound theorem to the simplicity of its statement. The straightforward implementation and the fast convergence of the procedure allow for the algorithm to be proposed as a handy tool for dealing with large truss-frame structures, endowed with several dofs, as well as for engineering designers who need fast comparisons among possible feasible structural choices. Moreover, no less importantly, the proposed algorithm reshapes an existing procedure for LA of a continuum to a discrete structural problem, suggesting in this way a methodological approach for transferring knowledge from a very experienced research field such as that of continuum LA, to a LA structural context, with new and much convenient results, overcoming those of traditional methods in that field.

The paper is structured as follows. Section 2 describes the proposed LA procedure. Specifically, after the kinematic description of the problem, the definition of the power produced by the external loads, the statement of the internal energy dissipation of the

structure and the analytical treatment of the interaction domain for the generic beam cross-section, the LA problem is formalized and the description of the iterative procedure is pointed out. Finally, the proof of convergence of the iterative procedure is provided. Section 3 illustrates the results of the numerical analyses conducted on benchmark structures, which have been performed with the implemented algorithm. Brief comments on various computational aspects and effectiveness of the simulations are concisely pointed out in closing Section 4.

Matrix notation is adopted throughout. Matrices and vectors are denoted by bold-face symbols. Transposition is indicated by

symbol T . A dot marks a time rate, i.e. a derivative with respect to an ordering time variable t .

2. Formulation and general framing of the procedure

2.1. Kinematic description of the problem

Let a structure be discretized by straight beam elements, with a uniform cross section and homogeneous material properties. Moreover, let each beam element of length L be described by a local reference system with axes x_1, x_2 and x_3, x_1 being the coordinate measured along the beam axis (see Fig. 1).

The degrees of freedom (dofs) governing the generic beam mechanism are selected as the 3 displacements and the 3 rotations in each of the two nodes at the beam edges, the absolute axial displacement and the absolute axial rotation of the inner part of the beam (between the two joints, see Fig. 1), totaling to 14 dofs for each beam element. The permanent kinematic discontinuities in the beam, commonly referred to as “generalized plastic strains”, are assumed to be concentrated in the so-called “plastic joints”, at the beam edges. These consist of the axial and the transverse relative rotations (ψ) and the axial relative displacement (η) for each joint (see Fig. 2), totaling to 8 plastic variables for each beam element. Negligible shear strain effects are assumed (slender beam elements).

According to such plastic mechanisms, by the principle of superposition of effects, the generalized plastic strains of the r -th beam element (Fig. 2) can be related to the dofs of the same beam element (Fig. 1) through the following kinematic relation:

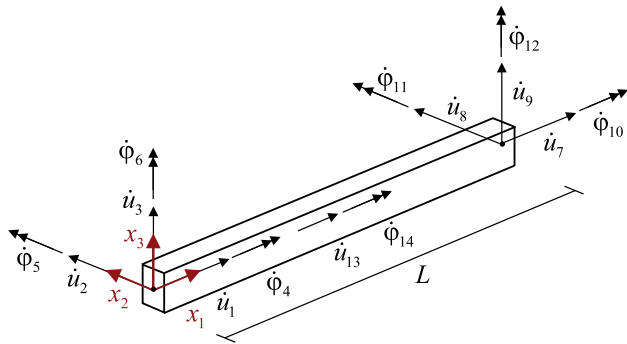


Fig. 1. Local reference system and kinematic variables (rates) adopted for the description of the beam element.

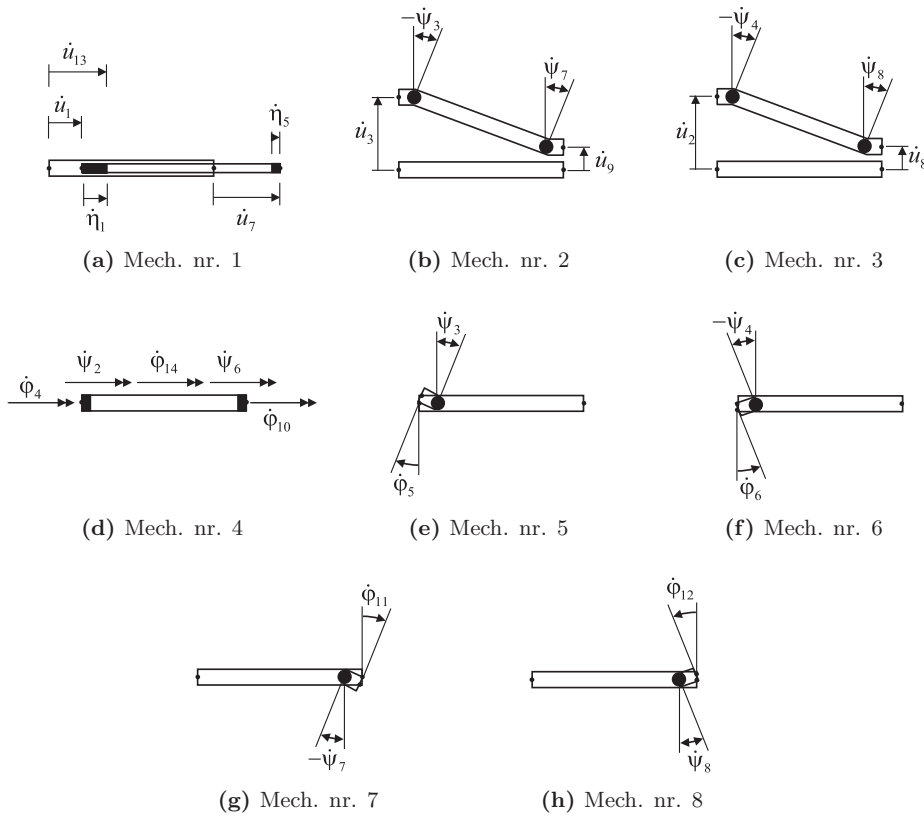


Fig. 2. Set of assumed (basic) plastic beam mechanisms.

$$\begin{bmatrix} \dot{\eta}_1 \\ \psi_2 \\ \psi_3 \\ \psi_4 \\ \dot{\eta}_5 \\ \psi_6 \\ \psi_7 \\ \psi_8 \end{bmatrix} = \underbrace{\begin{bmatrix} -1 & 0 & 0 & 0 & 0 & 0 & 0 & 0 & 0 & 0 & 0 & 0 & 1 & 0 \\ 0 & 0 & 0 & -1 & 0 & 0 & 0 & 0 & 0 & 0 & 0 & 0 & 0 & 1 \\ 0 & 0 & -1/L & 0 & 1 & 0 & 0 & 0 & 1/L & 0 & 0 & 0 & 0 & 0 \\ 0 & -1/L & 0 & 0 & 0 & -1 & 0 & 1/L & 0 & 0 & 0 & 0 & 0 & 0 \\ 0 & 0 & 0 & 0 & 0 & 0 & 1 & 0 & 0 & 0 & 0 & 0 & -1 & 0 \\ 0 & 0 & 0 & 0 & 0 & 0 & 0 & 0 & 0 & 1 & 0 & 0 & 0 & -1 \\ 0 & 0 & 1/L & 0 & 0 & 0 & 0 & 0 & -1/L & 0 & -1 & 0 & 0 & 0 \\ 0 & 1/L & 0 & 0 & 0 & 0 & 0 & -1/L & 0 & 0 & 0 & 1 & 0 & 0 \end{bmatrix}}_{\mathbf{B}_r} \begin{bmatrix} \dot{u}_1 \\ \dot{u}_2 \\ \dot{u}_3 \\ \phi_4 \\ \phi_5 \\ \phi_6 \\ \dot{u}_7 \\ \dot{u}_8 \\ \dot{u}_9 \\ \phi_{10} \\ \phi_{11} \\ \phi_{12} \\ \dot{u}_{13} \\ \phi_{14} \end{bmatrix} \quad (1)$$

where, related to the r -th beam element, vector $\dot{\eta}_r$ collects the generalized plastic strains and vector $\dot{\mathbf{u}}_r$ lists the dofs of the beam. Matrix \mathbf{B}_r represents the “generalized compatibility matrix” for the r -th beam element. It depends only on geometrical parameters and it is a sparse matrix.

If a global reference system (x, y, z) is adopted, “new” (global) dofs of r -th beam element $\dot{\mathbf{q}}_r$ can be related to local ones $\dot{\mathbf{u}}_r$ through orthogonal rotation matrix \mathbf{Q}_r , as follows:

$$\mathbf{R} = [\mathbf{e}_1 \mid \mathbf{e}_2 \mid \mathbf{e}_3], \quad \mathbf{Q}_r = \begin{bmatrix} \mathbf{R} & 0 & 0 & 0 & 0 \\ 0 & \mathbf{R} & 0 & 0 & 0 \\ 0 & 0 & \mathbf{R} & 0 & 0 \\ 0 & 0 & 0 & \mathbf{R} & 0 \\ 0 & 0 & 0 & 0 & \mathbf{I}_2 \end{bmatrix}^T, \quad \dot{\mathbf{u}}_r = \mathbf{Q}_r \dot{\mathbf{q}}_r \quad (2)$$

where orthogonal matrix \mathbf{R} is a rotation matrix (\mathbf{e}_j represents the versor of the j -th local axis of the r -th beam element). It is worth to note that no projection is required for the two last (internal) dofs of the r -th beam element (\mathbf{I}_2 being the 2×2 identity matrix).

Then, Eq. (1) becomes:

$$\dot{\eta}_r = \mathbf{B}_r \dot{\mathbf{u}}_r = \mathbf{B}_r \mathbf{Q}_r \dot{\mathbf{q}}_r = \bar{\mathbf{B}}_r \dot{\mathbf{q}}_r, \quad \bar{\mathbf{B}}_r = \mathbf{B}_r \mathbf{Q}_r \quad (3)$$

In describing the whole structure, supposed to be discretized in E elements and N nodes, vector $\dot{\eta}$ collects all the $8 \times E$ generalized plastic strains and vector \mathbf{q} lists all the dofs of the structure, of a number equal to $G = 6 \times N + 2 \times E$. Global “generalized compatibility matrix” \mathbf{B} is then built by assembling matrices \mathbf{B}_r by columns. It is worth noting that \mathbf{B} is a sparse matrix, with a quite low density of non-zero terms, not greater than $46 \times E$ over $8 \times E \times G$ total entries (i.e., less than an average of 6 non-zero terms in each row):

$$\dot{\eta} = \begin{bmatrix} \dots \\ \dot{\eta}_{r-1} \\ \dot{\eta}_r \\ \dots \end{bmatrix} = \mathbf{B} \dot{\mathbf{q}}, \quad \mathbf{B} = \begin{bmatrix} \dots & \dots & \dots & \dots & \dots \\ 0 & \bar{\mathbf{B}}_{r-1} & 0 & 0 & \dots \\ 0 & 0 & 0 & \bar{\mathbf{B}}_r & \dots \\ \dots & \dots & \dots & \dots & \dots \end{bmatrix} \quad (4)$$

2.2. Power produced by external actions

Let the structure be subjected to both permanent and live loads. Once defined a generic structural mechanism (\mathbb{M}), the work rate

produced by the external forces (\dot{L}_e) can be described by the following expression:

$$\dot{L}_e = \mu_k \dot{L}_e^0 + \dot{L}_e^g \quad (5)$$

where μ_k and \dot{L}_e^0 represent the (kinematic) load multiplier and the power of the base live loads, respectively; \dot{L}_e^g is the power produced by the permanent loads.

A structural mechanism can be assumed as a possible collapse mechanism when it is kinematically admissible, namely when the rigid body movement (velocity field) of each part of the structure is compatible with those of the other parts and the external power of the base live loads is positive ($\dot{L}_e^0 > 0$). In this way, defining \mathbb{C} as the set of all compatible mechanisms, the set of all kinematically admissible mechanisms is given as:

$$\mathbb{K} = \{ \mathbb{M} \in \mathbb{C}, \dot{L}_e^0 > 0 \} \quad (6)$$

For the generic mechanism, kinematical admissibility is guaranteed by the assembly procedure of the beam elements and by compatibility Eq. (4), together with the condition of a positive power produced by the base live loads ($\dot{L}_e^0 > 0$).

For each beam element, the power produced by the live loads can be easily computed by considering the mechanisms shown in Fig. 2; for instance, when uniform distributed loads p_1, p_2 and p_3 and couples m_4, m_5 and m_6 are applied along reference local axes x_1, x_2 and x_3 of the r -th beam element, respectively, it results:

$$\begin{aligned} (\dot{L}_e)_r &= p_1 \dot{u}_{13} L + p_2 \frac{\dot{u}_2 + \dot{u}_8}{2} L + p_3 \frac{\dot{u}_3 + \dot{u}_9}{2} L + \\ & m_4 \dot{\phi}_{14} L + m_5 \frac{\dot{u}_3 + \dot{u}_9}{L} L + m_6 \frac{\dot{u}_8 + \dot{u}_2}{L} L = \\ & = \left[0, \left(p_2 \frac{L}{2} - m_6 \right), \left(p_3 \frac{L}{2} + m_5 \right), 0, 0, 0, \dots \right. \\ & \left. 0, \left(p_2 \frac{L}{2} + m_6 \right), \left(p_3 \frac{L}{2} - m_5 \right), 0, 0, 0, (p_1 L), (m_4 L) \right] \dot{\mathbf{u}}_r = \mathbf{f}_r^T \dot{\mathbf{u}}_r \end{aligned} \quad (7)$$

where \mathbf{f}_r is the vector of nodal actions equivalent to the distributed loads considered applied on the r -th beam element. The representation of \mathbf{f}_r in the global reference system, i.e. $\hat{\mathbf{f}}_r$, is easily obtained too (see Eq. (2)):

$$(\dot{L}_e)_r = \mathbf{f}_r^T \dot{\mathbf{u}}_r = \mathbf{f}_r^T \mathbf{Q}_r \dot{\mathbf{q}}_r = (\mathbf{Q}_r^T \mathbf{f}_r)^T \dot{\mathbf{q}}_r = \hat{\mathbf{f}}_r^T \dot{\mathbf{q}}_r; \quad \hat{\mathbf{f}}_r = \mathbf{Q}_r^T \mathbf{f}_r \quad (8)$$

Analogous considerations can be stated for concentrated loads that may be applied along the beam and/or at the nodes.

Finally, considering \mathbf{T}_0 and \mathbf{T}_g as the vectors of the equivalent nodal actions produced by the assembly procedure and referred to live and permanent loads, respectively, it results:

$$\dot{L}_e^0 = \mathbf{T}_0^T \dot{\mathbf{q}}, \quad \dot{L}_e^g = \mathbf{T}_g^T \dot{\mathbf{q}} \quad (9)$$

2.3. Yield limit surfaces and internal power dissipation definition

As generally assumed in frame analysis, the activation of the limit plastic behavior in a plastic joint is ruled by a limit surface, defined in the space of the internal actions. In this context, the limit surface is represented by an uncoupled set of yield planes, each of them activating one of the 4×2 generalized plastic strains, namely a Rankine-type boxed-form yield domain (i.e. four couples of planes, each couple orthogonal to the axis of one static variable).

In each beam, two plastic joints are considered at the beam edges. The internal actions activating the plastic strains at each plastic joint are axial force, torque and two bending moments; shear effects are assumed to be negligible. Then, the analytical description of the interaction domain for each joint of a beam is stated in terms of the following inequalities:

$$\begin{cases} -N_L \leq (N_1, N_5) \leq +N_L \\ -M_{tL} \leq (M_2, M_6) \leq +M_{tL} \\ -M_{3L} \leq (M_3, M_7) \leq +M_{3L} \\ -M_{4L} \leq (M_4, M_8) \leq +M_{4L} \end{cases} \quad (10)$$

where N_1, N_5 are the axial forces, M_2, M_6 are the torques, M_3, M_4 and M_7, M_8 are the bending moments with respect to the two principal axes of inertia of the cross section, at the two edges of the beam, respectively. Yield limits $\pm N_L, \pm M_{tL}, \pm M_{3L}, \pm M_{4L}$ are assumed to be uniform along the beam.

By applying the normality flow rule, the internal power dissipation for the r -th beam element (\dot{d}_r) can be computed as:

$$\dot{d}_r = N_L |\dot{\eta}_1| + M_{tL} |\dot{\psi}_2| + M_{3L} |\dot{\psi}_3| + M_{4L} |\dot{\psi}_4| + N_L |\dot{\eta}_5| + M_{tL} |\dot{\psi}_6| + M_{3L} |\dot{\psi}_7| + M_{4L} |\dot{\psi}_8| \quad (11)$$

Consequently, the total internal power dissipation (\dot{L}_i) can be obtained by summing over the whole set of beam elements:

$$\dot{L}_i = \sum_{r=1}^M \dot{d}_r \quad (12)$$

It is worth noting that, when the generalized plastic strains are non-zero, the following quadratic form (which constitutes a main governing characteristics of the present LA kinematic formulation) may be given to the internal power dissipation:

$$\dot{d}_r = \frac{N_L}{|\dot{\eta}_1|} (\dot{\eta}_1)^2 + \frac{M_{tL}}{|\dot{\psi}_2|} (\dot{\psi}_2)^2 + \frac{M_{3L}}{|\dot{\psi}_3|} (\dot{\psi}_3)^2 + \frac{M_{4L}}{|\dot{\psi}_4|} (\dot{\psi}_4)^2 + \frac{N_L}{|\dot{\eta}_5|} (\dot{\eta}_5)^2 + \frac{M_{tL}}{|\dot{\psi}_6|} (\dot{\psi}_6)^2 + \frac{M_{3L}}{|\dot{\psi}_7|} (\dot{\psi}_7)^2 + \frac{M_{4L}}{|\dot{\psi}_8|} (\dot{\psi}_8)^2 \quad (13)$$

namely:

$$\dot{d}_r = \dot{\eta}_r^T \mathbf{M}_r(\dot{\eta}_r) \dot{\eta}_r \quad (14)$$

where:

$$\mathbf{M}_r(\dot{\eta}_r) = \text{diag} \left(\frac{N_L}{|\dot{\eta}_1|}, \frac{M_{tL}}{|\dot{\psi}_2|}, \frac{M_{3L}}{|\dot{\psi}_3|}, \frac{M_{4L}}{|\dot{\psi}_4|}, \frac{N_L}{|\dot{\eta}_5|}, \frac{M_{tL}}{|\dot{\psi}_6|}, \frac{M_{3L}}{|\dot{\psi}_7|}, \frac{M_{4L}}{|\dot{\psi}_8|} \right) \quad (15)$$

Finally, being \mathbf{M}_r a diagonal matrix, Eq. (12) becomes:

$$\dot{L}_i = \dot{\eta}^T \mathbf{M}(\dot{\eta}) \dot{\eta}, \quad \text{with } \mathbf{M}(\dot{\eta}) = \text{diag}(\dots, \mathbf{M}_{r-1}, \mathbf{M}_r, \dots) \quad (16)$$

2.4. Limit Analysis formulation

According to the upper-bound (kinematic) theorem of LA, a kinematic load multiplier μ_k is defined as follows:

$$\mu_k = \frac{\dot{L}_i - \dot{L}_e^g}{\dot{L}_e^0} \quad (17)$$

where \dot{L}_e^g and \dot{L}_e^0 have been introduced in Section 2.2 (see Eq. (5)); \dot{L}_i represents the internal power dissipation of the structure, previously defined by Eq. (16).

A corollary of the upper-bound theorem states that the collapse load multiplier is the minimum among the kinematic load multipliers computed for whole set \mathbb{K} of the kinematically admissible mechanisms:

$$\mu_c = \min_{\mathbb{K}} \{ \mu_k \} \quad (18)$$

Being \dot{L}_i and \dot{L}_e homogeneous functions of first order with respect to the velocity field, μ_k (Eq. (17)) is homogeneous of order zero and $\dot{L}_e^0 = 1$ can always be set for a kinematically admissible mechanism. Thus, the collapse load multiplier can be obtained as the solution to the following constrained optimization problem:

$$\mu_c = \min_{\mathbb{M} \in \mathbb{C}} \left\{ \dot{L}_i(\mathbb{M}) - \dot{L}_e^g(\mathbb{M}) \mid \dot{L}_e^0(\mathbb{M}) = 1 \right\} \quad (19)$$

If the minimization is limited to a subset of compatible mechanisms $\bar{\mathbb{C}} \subseteq \mathbb{C}$, it results:

$$\mu_c \leq \mu_k = \min_{\mathbb{M} \in \bar{\mathbb{C}}} \left\{ \dot{L}_i(\mathbb{M}) - \dot{L}_e^g(\mathbb{M}) \mid \dot{L}_e^0(\mathbb{M}) = 1 \right\} \quad (20)$$

For instance, with reference to the above structural discretization, this may happen when the collapse mechanism requires an active plastic joint within one or more beam elements, besides the plastic joints at the beam ends.

It is worth noting that, for practical applications, it is generally assumed that the collapse load multiplier is strictly positive, i.e. the structure is safe under permanent loads. However, this hypothesis is not required neither by the upper-bound theorem nor by the following discussion, so it will not be assumed in the sequel, namely the inequality in Eq. (20) holds true also for possible negative values of multipliers μ_c and μ_k .

2.5. Description of the iterative procedure for the kinematic Limit Analysis of frames

Constrained optimization problem (19) can be adapted to the frame kinematics, described in Section 2.1, by using vector $\dot{\mathbf{q}}$ to govern generic kinematically admissible mechanism $\mathbb{M} \in \mathbb{K}$. Kinematic admissibility requires the fulfillment of (homogeneous) kinematic boundary conditions. These last can be enforced, once for all, before the solution of optimization problem (20) by splitting vector $\dot{\mathbf{q}}$ into “constrained” ($\dot{\mathbf{q}}_0$) and “free” ($\dot{\hat{\mathbf{q}}}$) subsets:

$$\dot{\mathbf{q}} = \begin{bmatrix} \dot{\mathbf{q}}_0 \\ \dot{\hat{\mathbf{q}}} \end{bmatrix} = \underbrace{\begin{bmatrix} \mathbf{0} \\ \mathbf{I} \end{bmatrix}}_{\mathbf{W}} \dot{\hat{\mathbf{q}}} \quad (21)$$

Then, Eq. (4) becomes:

$$\dot{\eta} = \underbrace{\mathbf{B}\mathbf{W}}_{\hat{\mathbf{B}}} \dot{\hat{\mathbf{q}}} = \hat{\mathbf{B}} \dot{\hat{\mathbf{q}}} \quad (22)$$

and similar definitions arise for the vectors in Eq. (9):

$$\dot{L}_e^0 = \underbrace{\mathbf{T}_0^T \mathbf{W}}_{\hat{\mathbf{T}}_0^T} \dot{\mathbf{q}} = \hat{\mathbf{T}}_0^T \dot{\mathbf{q}}, \quad \dot{L}_g^0 = \underbrace{\mathbf{T}_g^T \mathbf{W}}_{\hat{\mathbf{T}}_g^T} \dot{\mathbf{q}} = \hat{\mathbf{T}}_g^T \dot{\mathbf{q}} \quad (23)$$

Thus the discretized version of problem (20) becomes:

$$\mu_c \leq \mu_k = \min_{\dot{\mathbf{q}}} \left\{ \dot{L}_i(\dot{\mathbf{q}}) - \hat{\mathbf{T}}_g^T \dot{\mathbf{q}} \mid \hat{\mathbf{T}}_0^T \dot{\mathbf{q}} = 1 \right\} \quad (24)$$

in which, considering Eq. (22):

$$\dot{L}_i(\dot{\mathbf{q}}) = \dot{\mathbf{q}}^T \mathbf{S}(\dot{\mathbf{q}}) \dot{\mathbf{q}}, \quad \mathbf{S}(\dot{\mathbf{q}}) = \hat{\mathbf{B}}^T \mathbf{M}(\dot{\mathbf{q}}) \hat{\mathbf{B}} \quad (25)$$

It is worth noting that matrix \mathbf{S} governs the global internal power dissipation of the structure, and it is straightforward to show that \mathbf{S} is symmetric, highly sparse (even narrow-banded with a proper numbering of dofs) and positive definite (or positive semi-definite when non-dissipative rigid-body motions are allowed by constraints), namely the same properties characterizing the classical global stiffness matrix for elastic FEM frame analysis. Note that when a node is common to e beam elements, in each one of the corresponding rows/columns there will be no more than $(8e + 6)$ non-zero entries.

In order to define the iterative algorithm, following the proposal by Zhang et al. [28] for the Limit Analysis of a two-dimensional rigid perfectly plastic body, at the beginning of the iterative process (i.e. at the initial step), vector $\dot{\mathbf{q}}_0$ is set up by a vector \mathbf{v} of random numbers and normalized in order to guarantee that $\hat{\mathbf{T}}_0^T \dot{\mathbf{q}}_0 = 1$:

$$\dot{\mathbf{q}}_0 = \frac{\mathbf{v}}{\hat{\mathbf{T}}_0^T \mathbf{v}} \quad (26)$$

Let one now consider iteration $n + 1$. Vector of nodal velocities $\dot{\mathbf{q}}_n$ relevant to the n -th iteration and corresponding load amplification factor μ_k^n are assumed to be known, the last one computed as follows:

$$\mu_k^n = \dot{L}_i(\dot{\mathbf{q}}_n) - \hat{\mathbf{T}}_g^T \dot{\mathbf{q}}_n = \dot{\mathbf{q}}_n^T \mathbf{S}_n \dot{\mathbf{q}}_n - \hat{\mathbf{T}}_g^T \dot{\mathbf{q}}_n, \quad \mathbf{S}_n = \mathbf{S}(\dot{\mathbf{q}}_n) \quad (27)$$

in which vector $\dot{\mathbf{q}}_n$ satisfies given constraint $\hat{\mathbf{T}}_0^T \dot{\mathbf{q}}_n = 1$.

Then, the iterative process leads to generate a new mechanism, governed by a new vector $\dot{\mathbf{q}}_{n+1}$ that is obtained as the solution of the following quadratic constrained minimization problem, in which coefficient matrix \mathbf{S}_n , computed in the previous iteration, is kept constant:

$$h_n(\dot{\mathbf{q}}_{n+1}) = \min_{\dot{\mathbf{q}}} \left\{ \dot{\mathbf{q}}^T \mathbf{S}_n \dot{\mathbf{q}} - 2\hat{\mathbf{T}}_g^T \dot{\mathbf{q}} \mid \hat{\mathbf{T}}_0^T \dot{\mathbf{q}} = 1 \right\} \quad (28)$$

The constrained minimization problem in Eq. (28) can be solved by enforcing the stationarity condition on the following Lagrange function:

$$H_n(\dot{\mathbf{q}}, \lambda) = \dot{\mathbf{q}}^T \mathbf{S}_n \dot{\mathbf{q}} - 2\hat{\mathbf{T}}_g^T \dot{\mathbf{q}} + 2\lambda(1 - \hat{\mathbf{T}}_0^T \dot{\mathbf{q}}) \quad (29)$$

where variable λ is a *Lagrangian multiplier*. The stationarity condition of $H_n(\dot{\mathbf{q}}, \lambda)$ leads to the following set of equations:

$$\begin{cases} \frac{\partial H_n}{\partial \dot{\mathbf{q}}} = 2\mathbf{S}_n \dot{\mathbf{q}} - 2\hat{\mathbf{T}}_g^T - 2\lambda \hat{\mathbf{T}}_0^T = \mathbf{0} \\ \frac{\partial H_n}{\partial \lambda} = 2(1 - \hat{\mathbf{T}}_0^T \dot{\mathbf{q}}) = 0 \end{cases} \quad (30)$$

Being, by assumption, non-dissipative rigid-body motions excluded by kinematic constraints, from Eq. (25) it results that $\dot{L}_i > 0$ for any $\dot{\mathbf{q}} \neq \mathbf{0}$, namely matrix \mathbf{S}_n is strictly positive definite (thus non-singular) and Eqs. (30a) can be solved for $\dot{\mathbf{q}}$, to get:

$$\dot{\mathbf{q}} = \mathbf{S}_n^{-1} (\hat{\mathbf{T}}_g + \lambda \hat{\mathbf{T}}_0) \quad (31)$$

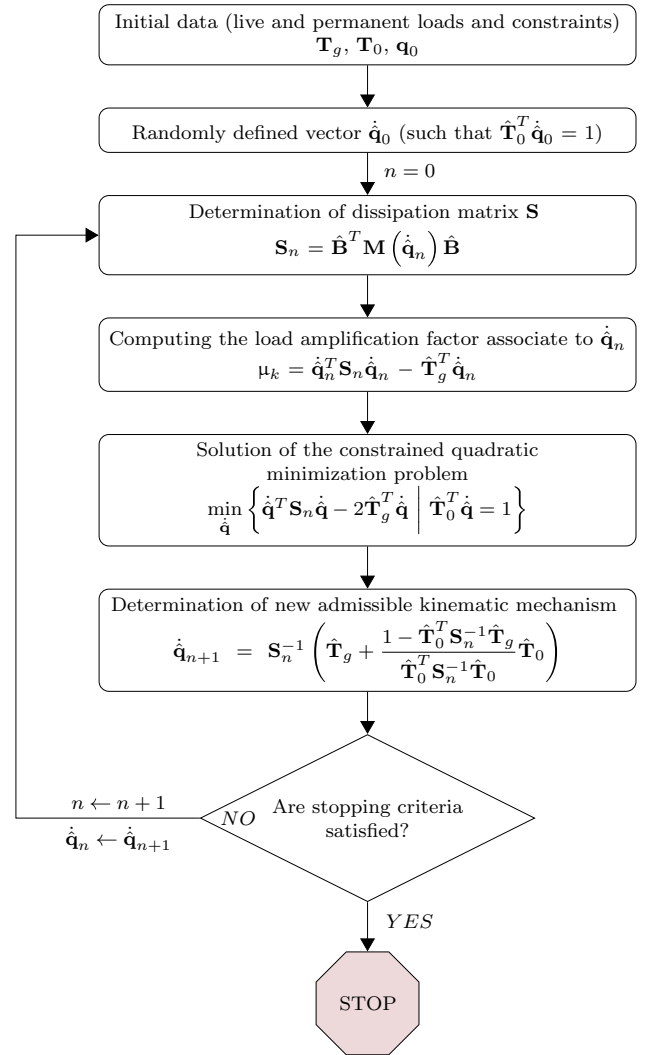


Fig. 3. Flow chart of the iterative algorithm.

By replacing Eq. (31) into Eq. (30b), Lagrangian multiplier λ_{n+1} is computed and then velocity vector $\dot{\mathbf{q}}_{n+1}$ is updated from Eq. (31) itself:

$$\lambda_{n+1} = \frac{1 - \hat{\mathbf{T}}_0^T \mathbf{S}_n^{-1} \hat{\mathbf{T}}_g}{\hat{\mathbf{T}}_0^T \mathbf{S}_n^{-1} \hat{\mathbf{T}}_0} \quad (32)$$

$$\dot{\mathbf{q}}_{n+1} = \mathbf{S}_n^{-1} (\hat{\mathbf{T}}_g + \lambda_{n+1} \hat{\mathbf{T}}_0) \quad (33)$$

Then, according to Eq. (27), a new kinematic load multiplier immediately follows:

$$\begin{aligned} \mu_k^{n+1} &= \dot{L}_i(\dot{\mathbf{q}}_{n+1}) - \hat{\mathbf{T}}_g^T \dot{\mathbf{q}}_{n+1} = \dot{\mathbf{q}}_{n+1}^T \mathbf{S}_{n+1} \dot{\mathbf{q}}_{n+1} - \hat{\mathbf{T}}_g^T \dot{\mathbf{q}}_{n+1}, \\ \mathbf{S}_{n+1} &= \mathbf{S}(\dot{\mathbf{q}}_{n+1}) \end{aligned} \quad (34)$$

The main steps of the iterative algorithm are schematically resumed in the flow-chart depicted in Fig. 3.

2.6. Proof of convergence of the iterative process

The algorithm illustrated in the previous section produces, in each iteration, a kinematic load multiplier that is not greater than

the previous one. The proof can be given by considering the following three inequalities.

The first one is obtained from Eq. (28), for which the minimization guarantees that:

$$h_n(\dot{\mathbf{q}}_{n+1}) = \dot{\mathbf{q}}_{n+1}^T \mathbf{S}_n \dot{\mathbf{q}}_{n+1} - 2\hat{\mathbf{T}}_g^T \dot{\mathbf{q}}_{n+1} \leq h_n(\dot{\mathbf{q}}_n) = \dot{\mathbf{q}}_n^T \mathbf{S}_n \dot{\mathbf{q}}_n - 2\hat{\mathbf{T}}_g^T \dot{\mathbf{q}}_n \quad (35)$$

Further, it can be underlined that the internal dissipated power for new mechanism $\dot{\mathbf{q}}_{n+1}$ can be expressed according to Eqs. (11) and (12), where the sum is explicitly extended to all the $8 \times E$ plastic modes (8 for each one of the E beam elements of the problem):

$$\dot{L}_i(\dot{\mathbf{q}}_{n+1}) = \dot{\mathbf{q}}_{n+1}^T \mathbf{S}_{n+1} \dot{\mathbf{q}}_{n+1} = N_L |\dot{\eta}_1|_{n+1} + M_{tL} |\dot{\psi}_2|_{n+1} + \dots + M_{4L} |\dot{\psi}_{8 \times E}|_{n+1} \geq 0 \quad (36)$$

It is also worth noting that Eq. (36) can be rewritten as follows:

$$\dot{L}_i(\dot{\mathbf{q}}_{n+1}) = \sqrt{\frac{N_L}{|\dot{\eta}_1|_n}} |\dot{\eta}_1|_{n+1} \sqrt{N_L |\dot{\eta}_1|_n} + \dots + \sqrt{\frac{M_{4L}}{|\dot{\psi}_{8 \times E}|_n}} |\dot{\psi}_{8 \times E}|_{n+1} \sqrt{M_{4L} |\dot{\psi}_{8 \times E}|_n} \quad (37)$$

or, equivalently:

$$\dot{L}_i(\dot{\mathbf{q}}_{n+1}) = \mathbf{z}^T \mathbf{p} \quad (38)$$

where

$$\mathbf{z} = \left[\sqrt{N_L |\dot{\eta}_1|_n}, \sqrt{M_{tL} |\dot{\psi}_2|_n}, \dots, \sqrt{M_{4L} |\dot{\psi}_{8 \times E}|_n} \right]^T, \quad \mathbf{p} = \left[\sqrt{\frac{N_L}{|\dot{\eta}_1|_n}} |\dot{\eta}_1|_{n+1}, \sqrt{\frac{M_{tL}}{|\dot{\psi}_2|_n}} |\dot{\psi}_2|_{n+1}, \dots, \sqrt{\frac{M_{4L}}{|\dot{\psi}_{8 \times E}|_n}} |\dot{\psi}_{8 \times E}|_{n+1} \right]^T \quad (39)$$

By applying the Cauchy-Schwarz inequality, a second inequality, in support of the proof of the algorithm convergence, is then provided:

$$0 \leq \dot{L}_i(\dot{\mathbf{q}}_{n+1}) = \mathbf{z}^T \mathbf{p} = |\mathbf{z}^T \mathbf{p}| \leq |\mathbf{z}| |\mathbf{p}| \quad (40)$$

in which:

$$|\mathbf{z}| = \sqrt{N_L |\dot{\eta}_1|_n + M_{tL} |\dot{\psi}_2|_n + \dots + M_{4L} |\dot{\psi}_{8 \times E}|_n} = \sqrt{\dot{L}_i(\dot{\mathbf{q}}_n)} = \sqrt{\dot{\mathbf{q}}_n^T \mathbf{S}_n \dot{\mathbf{q}}_n}, \quad |\mathbf{p}| = \sqrt{\frac{N_L}{|\dot{\eta}_1|_n} |\dot{\eta}_1|_{n+1}^2 + \frac{M_{tL}}{|\dot{\psi}_2|_n} |\dot{\psi}_2|_{n+1}^2 + \dots + \frac{M_{4L}}{|\dot{\psi}_{8 \times E}|_n} |\dot{\psi}_{8 \times E}|_{n+1}^2} = \sqrt{\dot{\mathbf{q}}_{n+1}^T \mathbf{S}_n \dot{\mathbf{q}}_{n+1}} \quad (41)$$

Now, let Eq. (34) be algebraically manipulated as follows:

$$0 \leq \dot{L}_i(\dot{\mathbf{q}}_{n+1}) = \dot{\mathbf{q}}_{n+1}^T \mathbf{S}_{n+1} \dot{\mathbf{q}}_{n+1} = \mu_k^{n+1} + \hat{\mathbf{T}}_g^T \dot{\mathbf{q}}_{n+1} \quad (42)$$

Eqs. (40)–(42) lead to:

$$0 \leq \dot{L}_i(\dot{\mathbf{q}}_{n+1}) = \mu_k^{n+1} + \hat{\mathbf{T}}_g^T \dot{\mathbf{q}}_{n+1} \leq |\mathbf{z}| |\mathbf{p}| = \sqrt{\dot{\mathbf{q}}_n^T \mathbf{S}_n \dot{\mathbf{q}}_n} \sqrt{\dot{\mathbf{q}}_{n+1}^T \mathbf{S}_n \dot{\mathbf{q}}_{n+1}} \quad (43)$$

Then, the algebraic manipulation of Eq. (27) gives:

$$0 \leq \dot{L}_i(\dot{\mathbf{q}}_n) = \dot{\mathbf{q}}_n^T \mathbf{S}_n \dot{\mathbf{q}}_n = \mu_k^n + \hat{\mathbf{T}}_g^T \dot{\mathbf{q}}_n \quad (44)$$

leading Eq. (42) to become:

$$0 \leq \dot{L}_i(\dot{\mathbf{q}}_{n+1}) = \mu_k^{n+1} + \hat{\mathbf{T}}_g^T \dot{\mathbf{q}}_{n+1} \leq |\mathbf{z}| |\mathbf{p}| = \sqrt{\mu_k^n + \hat{\mathbf{T}}_g^T \dot{\mathbf{q}}_n} \sqrt{\dot{\mathbf{q}}_{n+1}^T \mathbf{S}_n \dot{\mathbf{q}}_{n+1}} \quad (45)$$

Now, using the first inequality, Eq. (35), to obtain:

$$0 \leq \dot{\mathbf{q}}_{n+1}^T \mathbf{S}_n \dot{\mathbf{q}}_{n+1} \leq h_n(\dot{\mathbf{q}}_n) + 2\hat{\mathbf{T}}_g^T \dot{\mathbf{q}}_{n+1} = \dot{\mathbf{q}}_n^T \mathbf{S}_n \dot{\mathbf{q}}_n + 2\hat{\mathbf{T}}_g^T \dot{\mathbf{q}}_{n+1} - 2\hat{\mathbf{T}}_g^T \dot{\mathbf{q}}_n \quad (46)$$

and Eq. (44) to get:

$$0 \leq \dot{\mathbf{q}}_{n+1}^T \mathbf{S}_n \dot{\mathbf{q}}_{n+1} \leq \mu_k^n + 2\hat{\mathbf{T}}_g^T \dot{\mathbf{q}}_{n+1} - \hat{\mathbf{T}}_g^T \dot{\mathbf{q}}_n \quad (47)$$

Eq. (45) leads to the following final second inequality:

$$0 \leq \mu_k^{n+1} + \hat{\mathbf{T}}_g^T \dot{\mathbf{q}}_{n+1} \leq \sqrt{\mu_k^n + \hat{\mathbf{T}}_g^T \dot{\mathbf{q}}_n} \sqrt{\mu_k^n + 2\hat{\mathbf{T}}_g^T \dot{\mathbf{q}}_{n+1} - \hat{\mathbf{T}}_g^T \dot{\mathbf{q}}_n} \quad (48)$$

Finally, a third (last) inequality useful for proving the convergence of the proposed algorithm is based on the following special binomial product, valid for any couple of real values a and b :

$$(a - b)^2 \geq 0 \Rightarrow a^2 + b^2 - 2ab \geq 0 \Rightarrow b(2a - b) \leq a^2 \quad (49)$$

The last radicand in Eq. (48) can be rewritten as:

$$\mu_k^n + 2\hat{\mathbf{T}}_g^T \dot{\mathbf{q}}_{n+1} - \hat{\mathbf{T}}_g^T \dot{\mathbf{q}}_n = 2(\mu_k^n + \hat{\mathbf{T}}_g^T \dot{\mathbf{q}}_{n+1}) - (\mu_k^n + \hat{\mathbf{T}}_g^T \dot{\mathbf{q}}_n) \quad (50)$$

and variables a and b of Eq. (49) assume the following values:

$$a = \mu_k^n + \hat{\mathbf{T}}_g^T \dot{\mathbf{q}}_{n+1}, \quad b = \mu_k^n + \hat{\mathbf{T}}_g^T \dot{\mathbf{q}}_n \quad (51)$$

Eqs. (48) and (49) lead to obtain:

$$0 \leq \mu_k^{n+1} + \hat{\mathbf{T}}_g^T \dot{\mathbf{q}}_{n+1} \leq \sqrt{b} \sqrt{2a - b} \leq |a| = |\mu_k^n + \hat{\mathbf{T}}_g^T \dot{\mathbf{q}}_{n+1}| \quad (52)$$

In this case, exploiting the inequalities in Eqs. (44) and (47), it results:

$$2a - b \geq 0 \Rightarrow a \geq \frac{b}{2} \geq 0 \quad (53)$$

Then, from Eq. (52) the required evidence proof is finally derived:

$$\mu_k^{n+1} + \hat{\mathbf{T}}_g^T \dot{\mathbf{q}}_{n+1} \leq \mu_k^n + \hat{\mathbf{T}}_g^T \dot{\mathbf{q}}_{n+1} \Rightarrow \mu_k^{n+1} \leq \mu_k^n \quad (54)$$

namely, the new kinematic load multiplier is not greater than the previous one; equivalently, the kinematic load multipliers form a monotonic non-increasing sequence. Such a sequence is also bounded from below by collapse load multiplier μ_c and, then, it is convergent.

2.7. A remark on the implemented kinematic algorithm

From the description of the iterative procedure outlined in Section 2.5, it is noticeable that all the plastic modes in all the joints of the structure are active and remain active during the iterative process, namely all the strain variables assume a non-zero value in all the procedure steps (see e.g. Eqs. (15) and (33), where the strain rates appear as denominators and to be computed at the n^{th} iteration). However, some parts of the structure may not be involved in the collapse mechanism, or they may be involved just through rigid-body movements. In these parts, during the iterative procedure, the dissipation (and, then, the strain rates at the denominators in \mathbf{S}_n) will tend to vanish. As a consequence, due to computing round-off errors, governing matrix \mathbf{S}_n would become more and more ill-conditioned.

In order to avoid such an occurrence, a tolerance (tol) is ad hoc introduced to replace the generic denominator in \mathbf{S}_n when the computed value becomes lower than a pre-defined threshold. In particular, the following algorithm modification has been implemented, based on gained computational experience, in order to adequately run for different possible ranges of plastic deformation. Referring here as an example of description to the first plastic axial mode, by setting $\dot{\eta}_{max} = \max_i \{\dot{\eta}_i\}$, when it results that $|\dot{\eta}_1| < tol \dot{\eta}_{max}$, diagonal entry $M(1, 1)$ is set as:

$$M(1, 1) = \frac{N_L}{tol \dot{\eta}_{max}} \tag{55}$$

and the axial mode associated to $\dot{\eta}_1$ is registered as being “inactive”. The same applies to the diagonal entries associated to the other plastic modes.

By doing so, the convergence of the load multiplier sequence is no-longer monotonic and it may start oscillating. However, generally this happens when the kinematic load multiplier is already really very close to the collapse value, thus when final convergence is almost achieved. Despite that from various trial runs it has been experienced that values of the tolerance (*tol*) in the range of 10^{-9} – 10^{-4} yield to same final results in terms of convergence values, an appropriate value of tolerance is chosen here in such a way as to obtain only slight oscillations in the resulting plot of the load multiplier sequence. Specifically, in the subsequent applications, all runs have been performed with tolerance *tol* set to 10^{-7} .

In order to stop the procedure, two checks must be (both) verified: (i) the number of “inactive” modes has to remain constant for 10 iterations; (ii) the relative change of the load multiplier is lower than 10^{-3} .

3. Numerical tests

Out of several tested cases, four main numerical examples are presented and discussed in this section. Specifically, two initial examples refer to a simple space truss-frame cantilever beam, as basic reference tests; the other two examples analyze a six-story and a twenty-story space frame, whose computational results are available from the literature.

The first test, relevant to the cantilever beam, is strictly related to the flexural response of the beam; the second one to its torsional response. In both tests, the results are compared to the outcomes of analytical solutions, with a true perfect match.

The multi-story space frames have been considered as benchmark case studies for various algorithms of non-linear structural analysis (see e.g. Chiorean and Barsan [33], Van Long and Dang Hung [23] and references quoted therein). In particular, in the work by Van Long and Dang Hung [23], such frames have also been considered for testing an efficient algorithm for both limit and shakedown analysis of 3D frames by the kinematic method using a Linear Programming technique.

The following important remark applies. The results herein obtained for the multi-story frames are thereby compared to those earlier reported in Van Long and Dang Hung [23], even if there is no expectation of a strictly exact match. Indeed, different plastic domain and geometric non-linearity hypotheses are considered in Van Long and Dang Hung [23], as opposed to the formulation herein presented. Furthermore, an additional comparison is made to the elastoplastic formulation for non-linear evolutive structural analysis proposed in the earlier recent work by Ferrari et al. [31], with very satisfactory results. This last formulation consists of a step-by-step procedure apt to provide the “exact” collapse load multiplier, the configuration at incipient collapse and the collapse mechanism of general large-scale 3D truss-frame structures, in

which only material non-linearity is taken into account and a Rankine-type boxed-form yield domain is adopted (see also systematic application to a historical iron bridge structure in Ferrari et al. [30,32]).

In all the discussed examples, the analytical description of the interaction domain for the beam finite element is stated in terms of the inequalities reported in Section 2.3. Yield limits $N_L, M_{tL}, M_{3L}, M_{4L}$ are obtained from material yield limits σ_y, τ_y and cross section geometrical characteristics as:

$$N_L = A\sigma_y, \quad M_{3L} = Z_3\sigma_y, \quad M_{4L} = Z_4\sigma_y, \quad M_{tL} = Z_t\tau_y \tag{56}$$

where Z_3, Z_4 and Z_t are the plastic section moduli of each member, taken about the principal axes of inertia and the longitudinal axis of the beam, respectively.

3.1. Analyses of a truss-frame cantilever beam

Several trial structures have been considered for a first assessment. Results are here reported for a 3D truss-frame cantilever beam, as depicted in Fig. 4. Recalling the meaning of term truss-frame, as defined in the Introduction, notice that it refers here to the boxed-form, trusswork structure of the considered cantilever beam, potentially yielding also on the axial internal action, especially if just hinged nodes would be considered. Despite, in the simulations presented here, all the elements are considered to be encasted at the nodes, thus making it, truly speaking, a real frame in this sense.

Let one consider the cantilever beam as formed by ten equal cubic blocks, each one generated by beams of 1 m of length along each side. The material yield limits are $\sigma_y = 250$ MPa and $\tau_y = \sigma_y/\sqrt{3} = 144.3$ MPa; the plastic section moduli for the determination of the yield limits $N_L, M_{tL}, M_{3L}, M_{4L}$ are computed with reference to a square cross-section of a tubular beam, with 110 mm as external edge and 10 mm of thickness.

Specifically, the limit values of the internal actions read:

$$N_L = 1000 \text{ kN}, \quad M_{3L} = M_{4L} = 375.0 \text{ kN m}, \quad M_{tL} = 288.7 \text{ kN m} \tag{57}$$

In the first *bending test*, the structure is loaded by two vertical forces $\mu F, F = 100$ kN, acting downward at the free edge of the beam, one at each of the two top vertexes. The collapse mechanism obtained for this bending loading case is represented in Fig. 5. The associated numerical estimation of the collapse load multiplier is $\mu_k = 1.751 \geq \mu_c$.

In this case, the analytical computation of the collapse load can be easily performed according to the collapse mechanism suggested in Fig. 5, in which in the 4 joints closer to the cantilever constraints both axial and bending modes are active, while in each of the other 4 spotted joints only the axial mode is active. The remaining 9 blocks are subjected to the same rigid-body motion.

In order to describe a set of kinematically admissible mechanisms including a subset of collapse mechanisms, only the 4 joints closer to the constraints are assumed to be active and two global kinematic variables are chosen for the rigid block movement

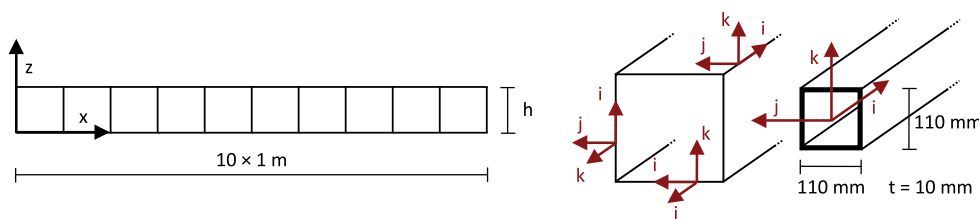


Fig. 4. Section orientations for the space truss-frame cantilever beam.

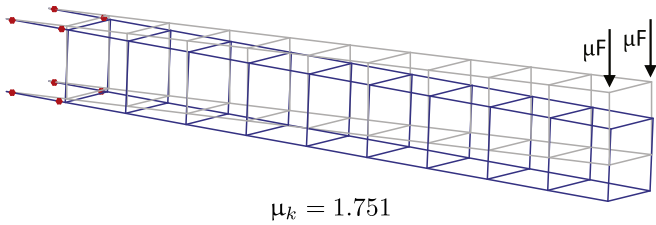


Fig. 5. Collapse mechanism of the truss-frame cantilever beam under bending.

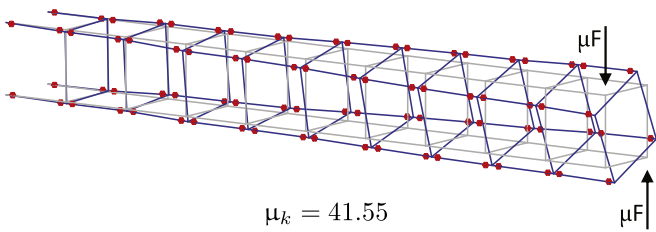


Fig. 6. Collapse mechanism of the truss-frame cantilever beam under torsion.

description: the horizontal movement (η) and the rotation (ψ) around the horizontal axes located at half height ($h/2$) between the constraints.

The axial elongations of the two upper beams and the two lower beams, respectively, are given as:

$$\dot{\eta}^+ = \dot{\eta} + \frac{h}{2}\dot{\psi}, \quad \dot{\eta}^- = \dot{\eta} - \frac{h}{2}\dot{\psi} \quad (58)$$

The internal power dissipation and the power produced by the base loads for this collapse mechanism are easily computed:

$$\dot{L}_i = 2N_L|\dot{\eta}^+| + 2N_L|\dot{\eta}^-| + 4M_L|\dot{\psi}|, \quad \dot{L}_e^0 = 2FL\dot{\psi} \quad (59)$$

Then, the kinematic load multiplier is computed as:

$$\mu_k = \min_{\dot{\eta}, \dot{\psi}} \left\{ \dot{L}_i \mid \dot{L}_e^0 = 1 \right\} \quad (60)$$

Table 1
Collapse load multipliers for the six-story frame.

Method	Limited M_{tL}	Unbounded M_{tL}	Limit state
Present kinematic	2.675	2.921	Formation of a mechanism
Evolutive LP [31]	2.675	2.921	First null eigv. of stiffness matrix
LA by LP [23]	-	2.412	Formation of a mechanism

namely as:

$$\mu_k = \min_{\dot{\eta}, \dot{\psi}} \left\{ 2N_L \left(\left| \dot{\eta} + \frac{h}{2}\dot{\psi} \right| + \left| \dot{\eta} - \frac{h}{2}\dot{\psi} \right| \right) + 4M_L|\dot{\psi}| \mid \dot{\psi} = \frac{1}{2FL} \right\} \quad (61)$$

$$\mu_k = \min_{\dot{\eta}} \left\{ 2N_L \left(\left| \dot{\eta} + \frac{h}{4FL} \right| + \left| \dot{\eta} - \frac{h}{4FL} \right| \right) + \frac{4M_L}{2FL} \right\} \quad (62)$$

$$\mu_k = 2N_L \frac{h}{2FL} + \frac{4M_L}{2FL} = \frac{N_L h + 2M_L}{FL} \geq \mu_c \quad (63)$$

In the equilibrium analysis, four limit couples M_{4L} (acting in vertical planes), two limit tensile axial forces N_L in the two upper joints and two limit compression axial forces N_L in the two lower joints are considered. Global equilibrium gives:

$$2N_L h + 4M_L - 2\mu_s FL = 0 \quad (64)$$

which can be solved for static load multiplier μ_s to give:

$$\mu_s = \frac{N_L h + 2M_L}{FL} \leq \mu_c \quad (65)$$

Thus, load multiplier μ_s represents a lower-bound to collapse load multiplier μ_c , because bending moments linearly decreasing from M_L to 0 can be assumed in the horizontal beams parallel to the frame main axis and nil bending moments are assigned to the beams transverse to the frame main axis. This static distribution fulfills both equilibrium and plastic consistency everywhere. So, it results:

$$\mu_c = \mu_s = \mu_k = \frac{N_L h + 2M_L}{FL} = 1.750 \text{ vs. } 1.751 \quad (66)$$

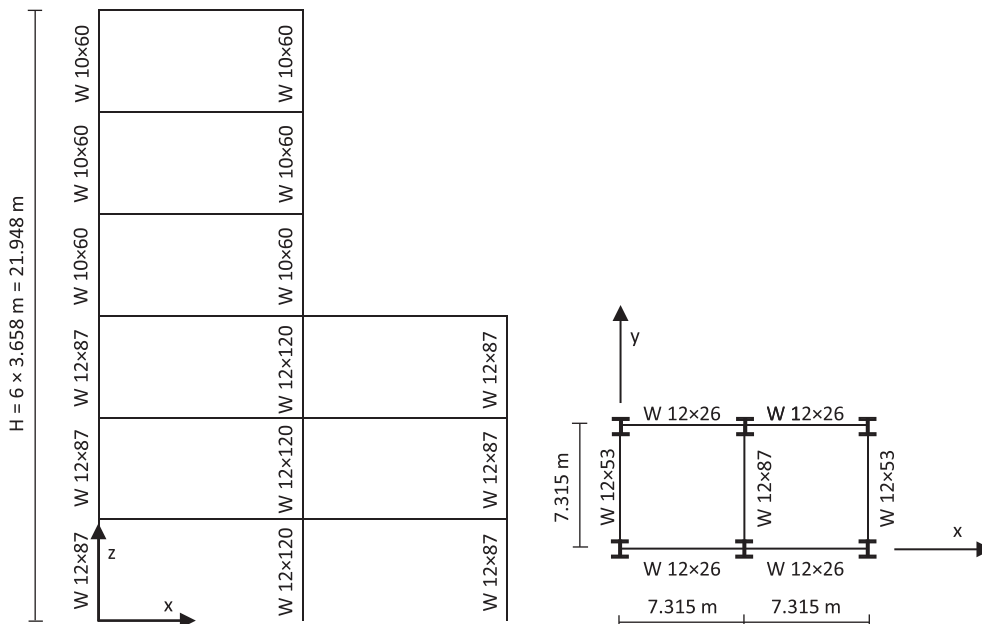


Fig. 7. Six-story frame.

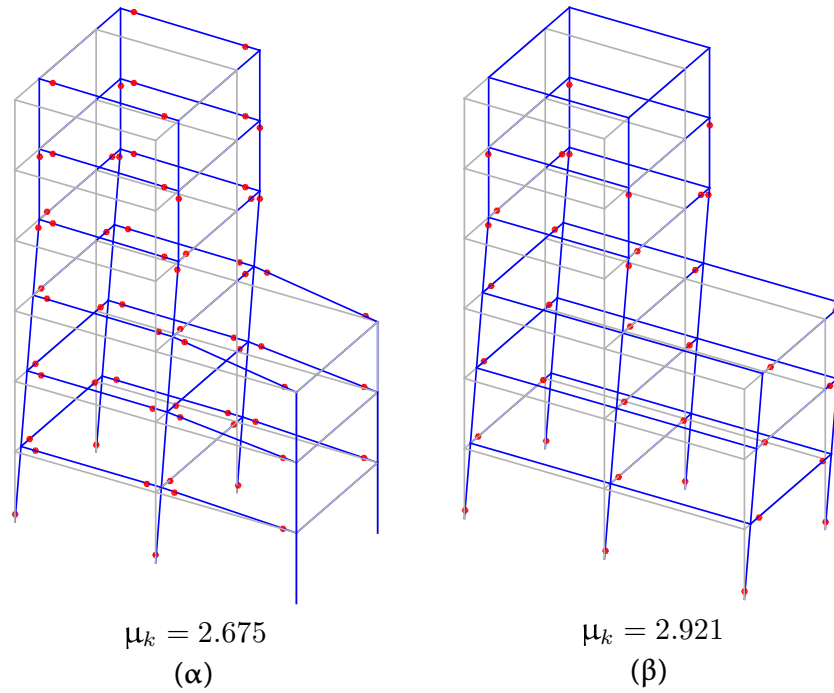


Fig. 8. Collapse mechanism of the six-story frame, (a) considering correct yield limit M_{tl} and (b) assuming an unbounded value of yield limit M_{tl} .

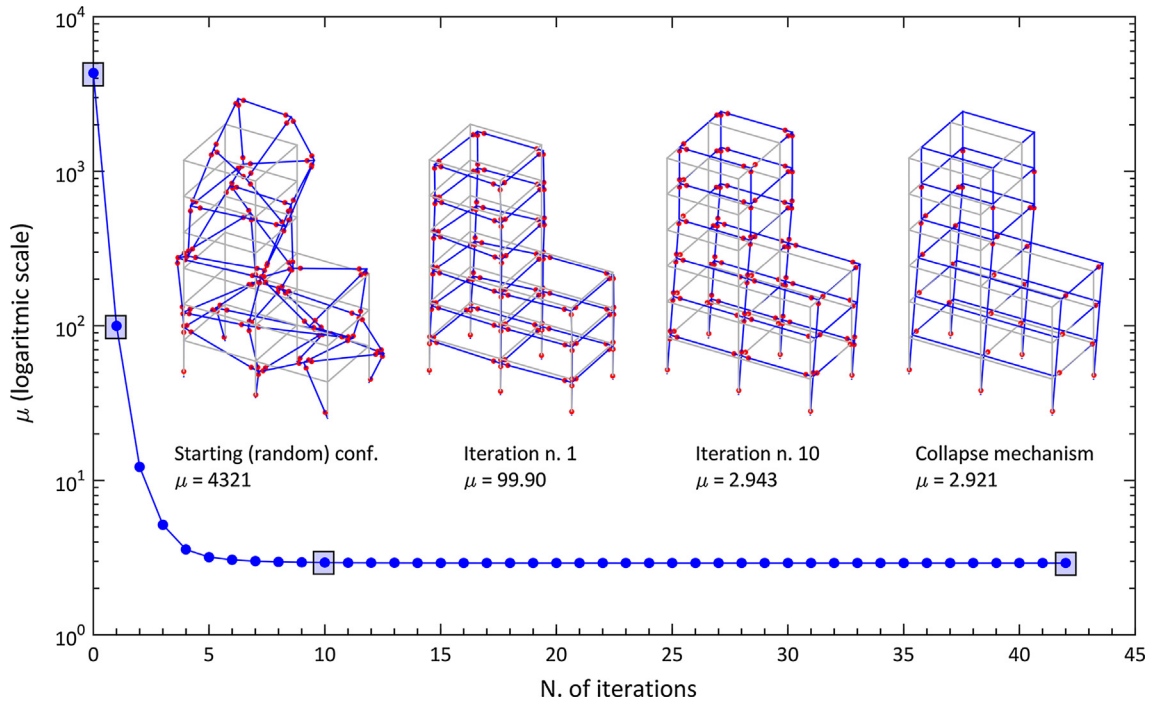


Fig. 9. Collapse load multiplier estimation during the iterative procedure, six-story frame.

Note that the computed minimum holds for any $|\dot{\eta}| \leq h/(4FL)$, namely the collapse load multiplier corresponds to a set of an infinite number of collapse mechanisms (actually obtained as a constrained linear combination of two basic mechanisms). However, such a multiplicity does not represent an obstacle for the above discussed numerical algorithm to fall down on μ_c .

A second *torsion test* is performed for the cantilever beam considering the structure to be loaded by two vertical forces $\mu F, F = 100$ kN, acting downward and upward, respectively, at the free edge of the beam; the resulting torque is $T = 100$ kN m.

The collapse mechanism obtained for this torsion loading case is represented in Fig. 6. In this case, the associated numerical estimation of the collapse load multiplier is $\mu_k = 41.55 \geq \mu_c$.

Analytically, the assumed kinematically admissible mechanism considers both the horizontal and vertical bending modes and the torsional mode as active in both joints of each beam parallel to the x axis. As (unique) degree of freedom, rigid (small) rotation ψ around the truss-frame axis of the four transverse beams at the truss-frame edge is adopted. By assuming that, for each set of four transverse beams, global rotation ψ is linearly decreasing down to

Table 2
Collapse load multipliers for the twenty-story frame.

Method	Limited M_{tl}	Unbounded M_{tl}	Limit state
Present kinematic	1.876	1.876	Formation of a mechanism
Evolutive LP [31]	1.876	1.876	First null eigv. of stiffness matrix
LA by LP [23]	–	1.698	Formation of a mechanism

zero along the truss-frame, the internal power and external power can be computed as follows:

$$\dot{L}_i = 40 \left(4M_L \frac{|\dot{\psi}|}{20} + M_{tl} \frac{|\dot{\psi}|}{10} \right), \quad \dot{L}_e^0 = F \frac{L}{10} \dot{\psi} \quad (67)$$

Then, the kinematic load multiplier associated with such a mechanism can be easily computed as:

$$\mu_k = \frac{\dot{L}_i}{\dot{L}_e^0} = 40 \frac{2M_L + M_{tl}}{FL} \geq \mu_c \quad (68)$$

For the equilibrium analysis, horizontal and vertical uniform shear forces $S_y = S_z = \pm 20M_L/L$ are assumed in all the beams parallel to the x axis, with equilibrium bending moments $M_3 = M_4 = \pm M_L$ and torque $M_2 = \pm M_{tl}$ at each beam edge.

The global equilibrium of the moments taken around the truss-frame axis gives:

$$4M_{tl} + 2S_y \frac{L}{10} + 2S_z \frac{L}{10} - \mu_s F \frac{L}{10} = 0 \quad (69)$$

and plastic consistency is everywhere fulfilled. Then, static multiplier μ_s can be obtained as:

$$\mu_s = 40 \frac{2M_L + M_{tl}}{FL} \leq \mu_c \quad (70)$$

The comparison of the two bounds in Eq. (68) and in Eq. (70) provides the collapse load amplification factor:

$$\mu_c = \mu_s = \mu_k = 40 \frac{2M_L + M_{tl}}{FL} = 41.55 \text{ vs. } 41.55 \quad (71)$$

3.2. Multi-story frames

Classical multi-story frames from the literature are now considered for further assessment and validation.

3.2.1. Six-story frame

The six-story frame is taken from Van Long and Dang Hung [23] and is depicted in Fig. 7. The structure is subjected to a uniform floor pressure of 4.8 kN/m², leading to consider a uniform distributed load of 64.2 kN/m along the spandrel beams and of 128.4 kN/m along the central beams. Wind load is represented by forces of 26.7 kN acting in the y -direction at every beam-column joint of the front elevation. Material yield limits are still taken as $\sigma_y = 250$ MPa and $\tau_y = \sigma_y/\sqrt{3} = 144.3$ MPa; the plastic section moduli for the determination of yield limits $N_L, M_{tl}, M_{3L,4L}$ refer to the AISC structural steel shapes reported in Fig. 7 itself.

The results obtained with the above-discussed numerical kinematic LA algorithm are shown in Table 1. In the same table, the results computed with the evolutive algorithm proposed in Ferrari et al. [31] and those taken from Van Long and Dang Hung [23] LP are listed for comparison purposes.

Two analyses have been performed, by considering the correct value M_{tl} or an unbounded value for the limit torsional moment. This is because in Van Long and Dang Hung [23] torsional effects have not been taken into account, while here they can either be accounted for or not.

The exact match between the collapse load multiplier obtained by the proposed algorithm and the one resulting from the piecewise linear elastoplastic step-by step analysis in Ferrari et al. [31] proves the efficiency of the LA procedure here presented. In the results shown by Van Long and Dang Hung [23], an expected gap can be observed: in fact, the collapse load multiplier obtained with the proposed algorithm is about 17% higher than the one computed in Van Long and Dang Hung [23]. This is due to the fact that the (piece-wise linear) yield domain used in the latter reference work is included in the Rankine-type boxed-form here adopted.

Fig. 8 shows the collapse mechanisms for the two cases referred to in Table 1, respectively. As the loads and structure are asymmetrical, torsional effects are induced and the frame deforms in a twisting mode. Obviously, this behavior results to be more evident in Case (a), in which yield limits M_{tl} are considered within the yield domain definition. In this case, the collapse mechanism is indeed characterized by a higher number of active joints, symbolically depicted in Fig. 8 by red spots.

For Case (b) in Fig. 8, Fig. 9 illustrates the performance of the iterative algorithm. It shows the collapse load multiplier computed

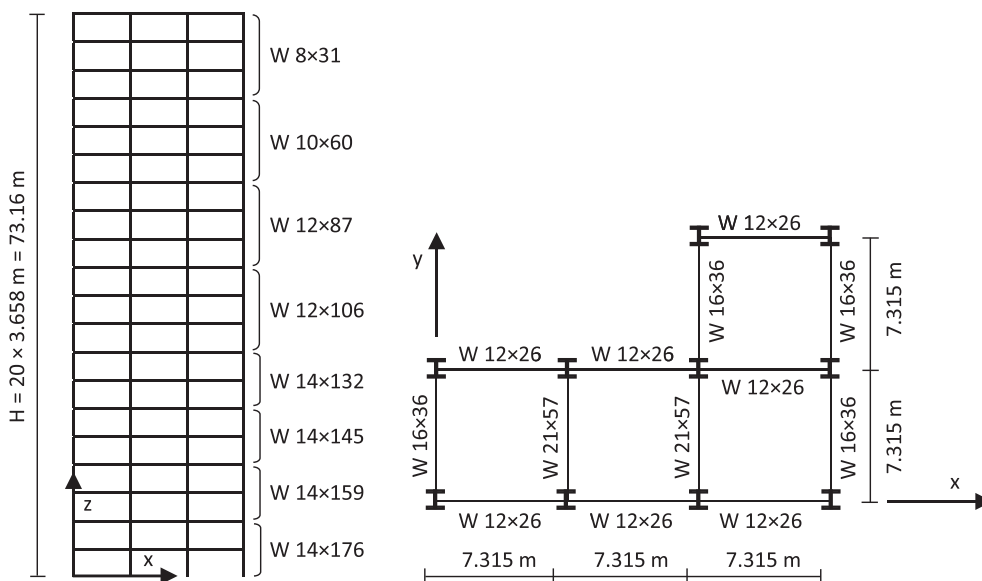


Fig. 10. Twenty-story frame.

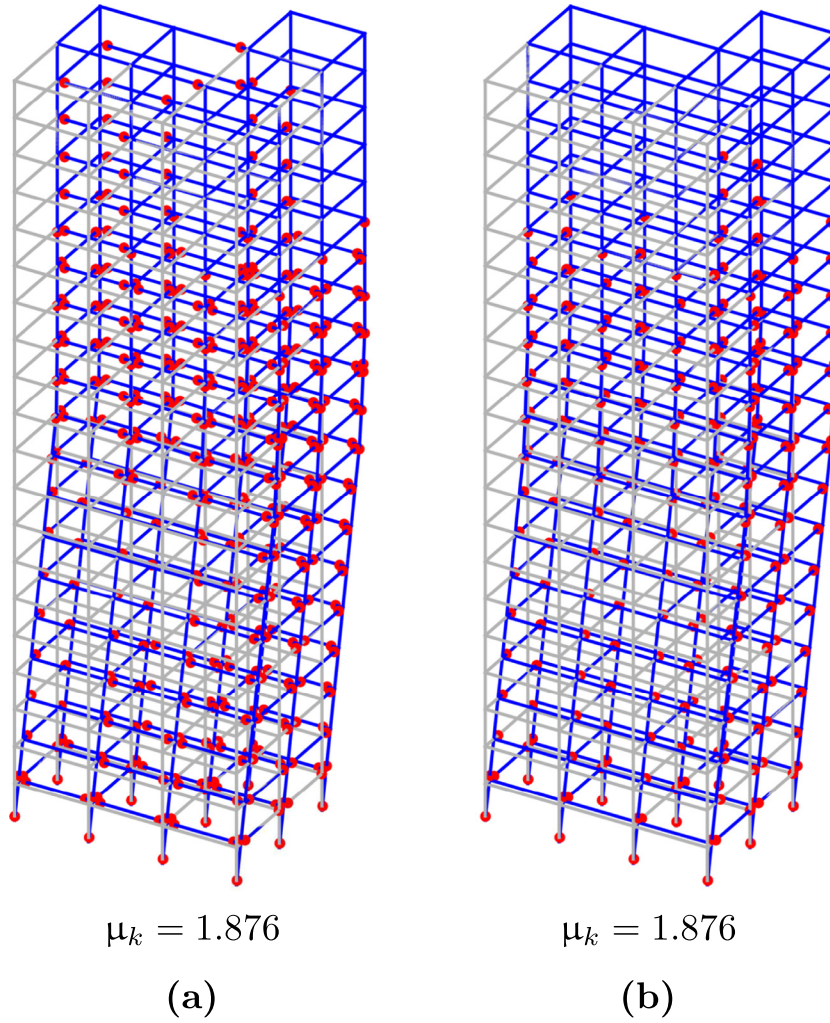


Fig. 11. Collapse mechanism of the twenty-story frame, (a) considering correct yield limit M_u and (b) assuming an unbounded value of yield limit M_u .

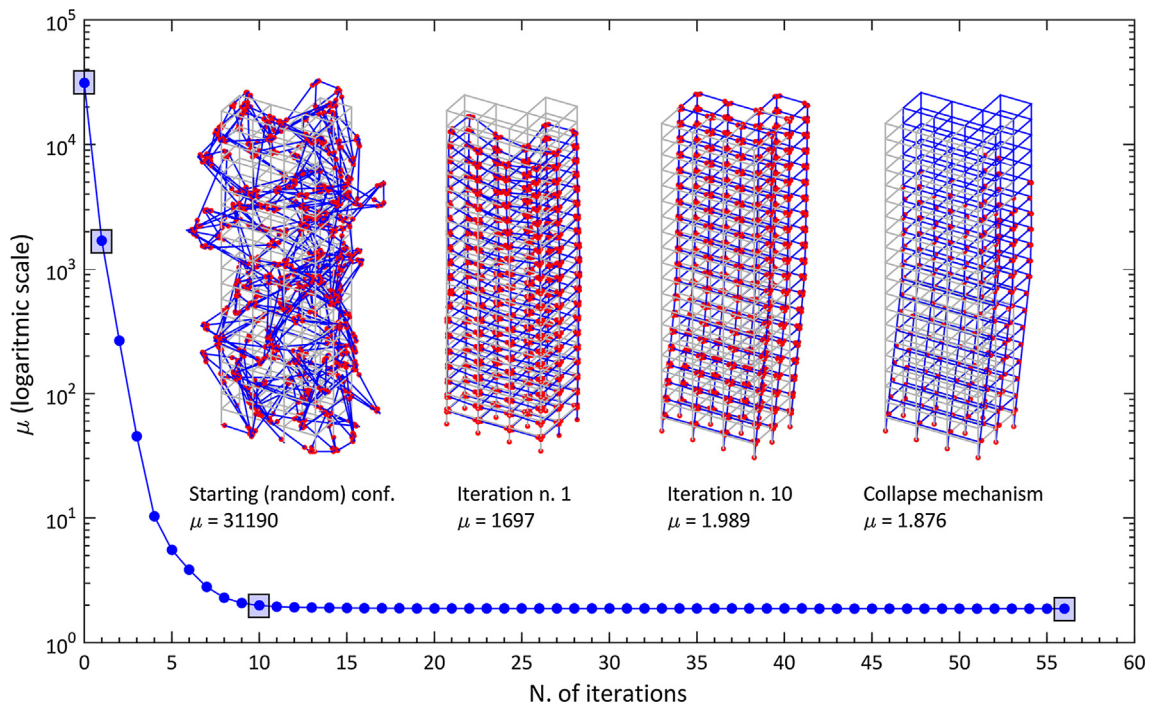


Fig. 12. Collapse load multiplier estimation during the iterative procedure, twenty-story frame.

during the iterative procedure. In the picture, it is possible to appreciate how the implemented algorithm is able to quickly and easily achieve convergence. In fact, the collapse mechanism is almost already achieved at the first iteration, and in just 10 iterations the expected value of the collapse load multiplier is practically obtained (with a relative error of about 0.8%); after that, the trend of kinematic multiplier μ_k becomes almost flat at increasing number of iterations. In this case, the computing time to get the solution (in 42 iterations) was less than 0.6 s. The algorithm has been implemented and run as a non-compiled (interpreted) code within MATLAB®, under a Windows 10 operating system, on a Dell laptop endowed with an Intel Core i7-6500U Processor, clock at 2.50 GHz and 16 GB RAM. As a comparison reference on computational burden and performance, similar characteristic data have been recorded for the same structure, by a different SOCP (see Introduction) elastoplastic Limit Analysis and Shakedown method in the above-cited work of Skordeli and Bisbos [35], in 2010 (see their Table 2). As a further reference on the same present hardware platform as described above, the computing time recorded to get convergence, though for a full evolutive elastoplastic analysis up to collapse as proposed in Ferrari et al. [31] (see Table 1), was recorded in about 6 s.

3.2.2. Twenty-story frame

The last example is the 3D twenty-story frame taken from the work of Van Long and Dang Hung [23] and depicted in Fig. 10. The structure is loaded by a uniform floor pressure of 4.8 kN/m², leading to consider a uniform distributed load of 64.2 kN/m along the spandrel beams and of 128.4 kN/m along the central beams. A wind pressure of 0.96 kN/m² is simulated by point loads acting in the y-direction at every beam-column joint of the front elevation. The material yield limits are taken as $\sigma_y = 344.8$ MPa and $\tau_y = \sigma_y/\sqrt{3} = 199.1$ MPa; the plastic section moduli for the determination of yield limits $N_L, M_{1L}, M_{3L,4L}$ refer to the AISC structural steel shapes reported in Fig. 10 itself.

The results obtained by the present kinematic LA approach are shown in Table 2, along with those obtained by using the evolutive algorithm proposed in Ferrari et al. [31] and from Van Long and Dang Hung [23] LP. Comparisons have been made for the same two yielding cases considered for the six-story frame.

Also in this case, an exact match has been obtained with the collapse load computed by the step-by-step algorithm presented in Ferrari et al. [31], for both the considered cases. Remarks analogous to those stated in Section 3.2.1, for the comparison with the results presented in Van Long and Dang Hung [23], could be repeated. In this case, a smaller variation (about 9%) of the collapse load amplifier has been obtained, still consistent with a wider Rankine boxed-form yield domain here taken.

In Fig. 11 the collapse mechanisms for the two cases listed in Table 2 are represented. The two collapse load amplifiers differ only after the fourth significant digits; the two collapse mechanisms appear to be very similar to each other but, as it happens in Section 3.2.1, Case (b) shows a lower number of active joints. This suggests that, under the considered load distribution, in this example, the torsional strength of the beams does not significantly affect the collapse of the structure.

As given for the six-story frame case, Fig. 12 shows the collapse load multipliers computed during the iterative procedure (collapse mechanism in Fig. 11, Case (b)). Also in this case, the collapse mechanism is almost already achieved after about 10 iterations; the expected value of the collapse load multiplier is practically obtained (relative error of about 1.2%) at around the 15th iteration. To get convergence (in 56 iterations), the computing time was recorded as less than 4 s. As a matter of fact, Orbison et al. [38], in 1982, for the same structure, but accounting for a non-linear

kinematics, a more sophisticated yield surface and a non-comparable hardware (a VAX minicomputer), computed the collapse load with a step-by-step procedure in 14 minutes. Moreover, the full evolutive elastoplastic analysis by Ferrari et al. [31], as also quoted earlier, requires here 80 s of analysis.

4. Conclusions

In the paper, an efficient approach for the kinematic LA of (3D) truss-frame structures has been presented. It is based on an existing approach for LA of (2D) continua and adapted to beams with a Rankine-type boxed-form yield domain. The iterative algorithm involved in the procedure is described in detail; the proof of convergence of the iterative process is provided.

Four numerical examples have been presented. The first two consist of a space truss-frame cantilever beam under bending and torsion, respectively. In these cases the effectiveness of the proposed algorithm is proven by the comparison between the results obtained from the proposed procedure and those coming from an analytically determined solution. These numerical tests deserve attention also for demonstrating the effectiveness of the algorithm in capturing the collapse load multiplier and one of the collapse mechanisms of the structure even in the presence of an infinite number of collapse mechanisms.

Then, the kinematic algorithm has been adopted for the LA of two multi-story 3D frame structures proposed in the literature, with available computational results. Moreover, results coming from an independent step-by-step evolutive approach have been computed for comparison purposes. The effectiveness of the proposed procedure turned out to be very satisfactory, considering both the available sets of results. The algorithm rapidly converges, with a kinematic multiplier quickly precipitating toward the sought collapse load multiplier, illustrating the feasibility and convenience of this new algorithm.

The proposed kinematic LA approach is meant to be a handy tool for designers to provide fast comparisons among different structural choices, particularly because of its straightforward implementation and displayed fast convergence. Mainly for this reason, the procedure may constitute a key tool for effectively handling even very large truss-frame structures, endowed with a high number of dofs, with quick and affordable estimations of the potential collapse characteristics, apt to possibly reiterate the design concept in view of a structural performance optimization.

Indeed, about future perspective implications of Limit Analysis, in general terms and in terms of the present specific LA investigation, within the realm of structural engineering, the following closing considerations may be in order. The present work has derived a new and elegant algorithm for the Limit Analysis of general truss-frame structures, by achieving a consistent and rapid kinematic prediction of the collapse load multiplier and of the associated collapse mechanism. Despite for the intrinsic limitations of the classical underlying hypotheses that are typical of LA (specifically perfectly elastoplastic response of each component and compact cross section shapes apt to prevent buckling of any form), within a monotonic static loading regime, the demonstrated efficiency of the new kinematic LA procedure may help in bringing new attention to the LA discipline within structural engineering. In fact, the proposed algorithm has been demonstrated to potentially present an interest in preliminary “form-finding” architectural and structural design. Furthermore, other implications may be read in the important perspective of seismic engineering design. Indeed, a particular application where collapse loads are of a major concern is represented by the field of earthquake-resistant structural design. Although there the whole dynamic response should actually need to be considered, the proposed LA collapse framework shows

strong compatibilities and interrelations with respect to that, in the perspective of possible design applications within that field. Moreover, although the collapse of buildings is certainly of a major safety concern, the serviceability of the structure often constitutes as well a governing design concept. For instance, in seismic design, the building functionality represents a major concern in ensuring life safety: such a functionality may be compromised at shaking levels that are still below collapse (non-structural components may fail, architectural parts may detach from the structural framework due to excessive drifts or displacements, building content may overturn, slide or detach, etc.). Thus, in the context of a genuine displacement- or performance-based design within such a frame, LA could indeed regain an important momentum within structural engineering, starting from new efficient LA procedures such as that put forward by the present research investigation (and also those referring to the separate, though much related evolutive elastoplastic studies recently reported in Ferrari et al. [30–32]).

Compliance with Ethical Standards

The authors declare that they have no conflict of interest.

Acknowledgments

This work has been carried-out at the University of Bergamo, Department of Engineering and Applied Sciences (Dalmine). The financial support by “Fondi di Ricerca d’Ateneo ex 60%” at the University of Bergamo is gratefully acknowledged.

Appendix A. Supplementary material

Supplementary data associated with this article can be found, in the online version, at <https://doi.org/10.1016/j.compstruc.2017.11.018>.

References

- [1] Drucker DC, Prager W, Greenberg HJ. Extended limit design theorems for continuous media. *Quart Appl Math*, Brown University 1952;9(4):381–9. <http://www.jstor.org/stable/43633923>.
- [2] Massonet CH, Save M. In: Nelissen B, editor. *Calcul Plastique des Constructions*. Belgium: Angleur, Liège; 1978.
- [3] Kaliszky S. *Plasticity: Theory and Engineering Applications*. Amsterdam, Netherlands: Elsevier; 1989.
- [4] Lubliner J. *Plasticity Theory*. New York: McMillan Publisher; 1990.
- [5] Jirasek M, Bazant ZP. *Inelastic Analysis of Structures*. Chichester, U.K: Wiley; 2002.
- [6] Spiliopoulos K, Weichert D. *Direct Methods for Limit States in Structures and Materials*. Dordrecht, Netherlands: Springer Science+Business Media; 2014.
- [7] Maier G. A matrix structural theory of piecewise-linear plasticity with interacting yield planes. *Meccanica* 1970;5(1):54–66.
- [8] Lysmer J. Limit analysis of plane problems in soil mechanics. *J Soil Mech Found Divis* 1970;96(4):1311–34.
- [9] Capurso M. Limit analysis of continuous media with piecewise linear yield condition. *Meccanica* 1971;6(1):53–8.
- [10] Anderheggen E, Knöpfel H. Finite element limit analysis using linear programming. *Int J Solids Struct* 1972;8(12):1413–31.
- [11] Christiansen E. Computation of limit loads. *Int J Numer Methods Eng* 1981;17(10):1547–70.
- [12] Andersen KD, Christiansen E. Limit analysis with the dual affine scaling algorithm. *J Comput Appl Math* 1995;59(2):233–43.
- [13] Andersen KD, Christiansen E, Overton ML. Computing limit loads by minimizing a sum of norms. *SIAM J Scient Comput* 1998;19(3):1046–62.
- [14] Christiansen E, Andersen KD. Computation of collapse states with von Mises type yield condition. *Int J Numer Methods Eng* 1999;46(8):1185–202.
- [15] Andersen KD, Christiansen E, Conn AR, Overton ML. An efficient primal-dual interior-point method for minimizing a sum of Euclidian norms. *SIAM J Scient Comput* 2000;22(1):243–62.
- [16] Zouain N, Herskovits J, Borges LA, Feijóo RA. An iterative algorithm for limit analysis with nonlinear yield functions. *Int J Solids Struct* 1993;30(10):1397–417.
- [17] Lyamin AV, Sloan SW. Lower bound limit analysis using non-linear programming. *Int J Numer Methods Eng* 2002;55(5):573–611.
- [18] Lyamin AV, Sloan SW. Upper bound limit analysis using linear finite elements and non-linear programming. *Int J Numer Anal Methods Geomech* 2002;26(2):181–216.
- [19] Ben-Tal A, Nemirovsky A. *Lectures on modern convex optimization: analysis, algorithms and engineering applications*. MOS–SIAM Series on Optimization, Philadelphia; 2001.
- [20] Ciria H, Pareire J. Computation of upper and lower bounds in limit analysis using second-order cone programming and mesh adaptivity. In: *Proc of 9th ASCE Speciality Conference on Probabilistic Mechanics and Structural Reliability (PMC2004)*, Albuquerque, New Mexico; 2004. p. 13.
- [21] Prager W. The theory of plasticity: a survey of recent achievements. *Proc Inst Mech Eng* 1955;169(1):41–57.
- [22] Nguyen-Dang H. CEPAO – an automatic program for rigid-plastic and elastoplastic analysis and optimization of frames structures. *Eng Struct* 1984;6(1):33–51.
- [23] Van Long H, Dang Hung N. Limit and shakedown analysis of 3D steel frames. *Eng Struct* 2008;30(7):1895–904.
- [24] Liew JYR, Chen H, Shanmugam NE, Chen WF. Improved nonlinear plastic hinge analysis of space frame structures. *Eng Struct* 2000;22(10):1324–38.
- [25] Liew JYR, Chen H, Shanmugam NE. Inelastic analysis of steel frames with composite beams. *J Struct Eng* 2001;127(2):194–202.
- [26] Cocchetti G, Maier G. Elastic-plastic and limit-state analyses of frames with softening plastic-hinge models by mathematical programming. *Int J Solids Struct* 2003;40(25):7219–44.
- [27] Tangaramvong S, Tin-Loi F. A complementarity approach for elastoplastic analysis of strain softening frames under combined bending and axial force. *Eng Struct* 2007;29(5):742–53.
- [28] Zhang P, Lu M, Hwang K. A mathematical programming algorithm for limit analysis. *Acta Mech Sin* 1991;7(3):267–74.
- [29] Zhang Y-G, Zhang P, Xue W-M. Limit analysis considering initial constant loadings and proportional loadings. *Comput Mech* 1994;14(3):229–34.
- [30] Ferrari R, Cocchetti G, Rizzi E. Elastoplastic structural analysis of the Paderno d’Adda bridge (Italy, 1889) based on Limit Analysis. In: *Proc of 8th Int Conf on Structural Analysis of Historic Constructions (SAHC2012)*, Ed. Jerzy Jasiński, Wrocław, Poland, October 15–17, 2012, DWE, Wrocław, Poland, ISSN: 0860-2395, ISBN: 978-83-7125-216-7, Vol. 3, pp. 2171–2180. Also published in *Wiadomości Konserwatorskie - Journal of Heritage Conservation*, Nr. 34/2013, pp. 28–35, ISSN: 0860-2395; 2012. <<http://www.skz.pl/portal/nowy/kontener/wk.htm>>, Stowarzyszenie Konserwatorów Zabytków - Association of Monument Conservators, Poland.
- [31] Ferrari R, Cocchetti G, Rizzi E. Limit Analysis of a historical iron arch bridge. Formulation and computational implementation. *Comput Struct* 2016;175(Oct):184–96. <https://doi.org/10.1016/j.compstruc.2016.05.007>.
- [32] Ferrari R, Cocchetti G, Rizzi E. Computational elastoplastic Limit Analysis of the Paderno d’Adda bridge (Italy, 1889). *Arch Civil Mech Eng* 2017;18(1):291–310. <https://doi.org/10.1016/j.acme.2017.05.002>.
- [33] Chiorean CG, Barsan GM. Large deflection distributed plasticity analysis of 3D steel frameworks. *Comput Struct* 2005;83(19–20):1555–71.
- [34] Lógó J, Kaliszky S, Hjiáj M, Movahredi Rad M. Plastic Limit and Shakedown Analysis of Elasto-plastic Steel Frames with Semirigid Connections. In: Károly Jármai, József Farkas, editors. *Proc of Design, Fabrication and Economy of Welded Structures*. Miskolc, Hungary; April 24–26, 2008. p. 237–44.
- [35] Skordeli M-AA, Bisbos CD. Limit and shakedown analysis of 3D steel frames via approximate ellipsoidal yield surfaces. *Eng Struct* 2010;32(6):1556–67.
- [36] Bleyer J, Buhan P. Yield surface approximation for lower and upper bound yield design of 3D composite frame structures. *Comput Struct* 2013;129(December):86–98.
- [37] Nikolaou KD, Georgiadis K, Bisbos CD. Lower bound limit analysis of 2D steel frames with foundation-structure interaction. *Eng Struct* 2016;118(July):41–54.
- [38] Orbison JG, McGuire W, Abel JF. Yield surface applications in nonlinear steel frame analysis. *Comput Methods Appl Mech Eng* 1982;33(1–3):557–73.